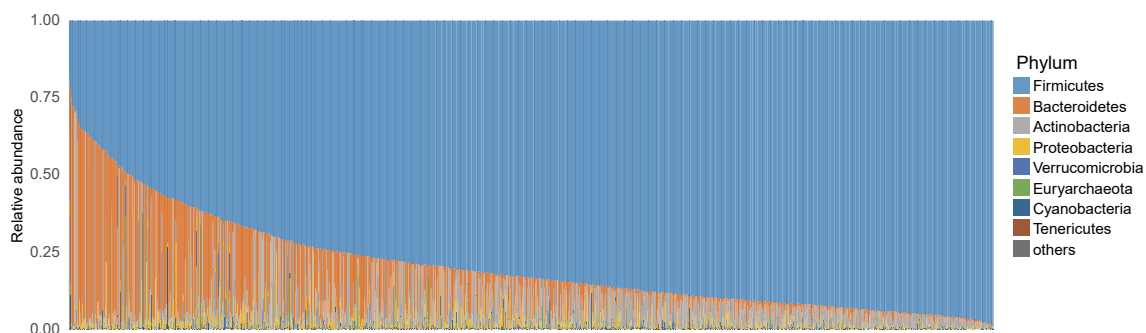
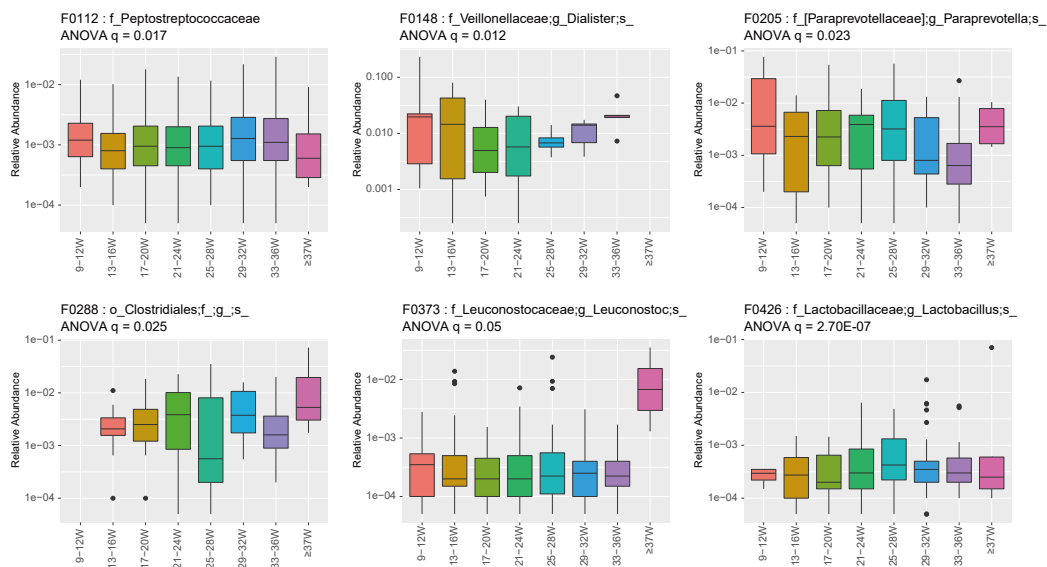


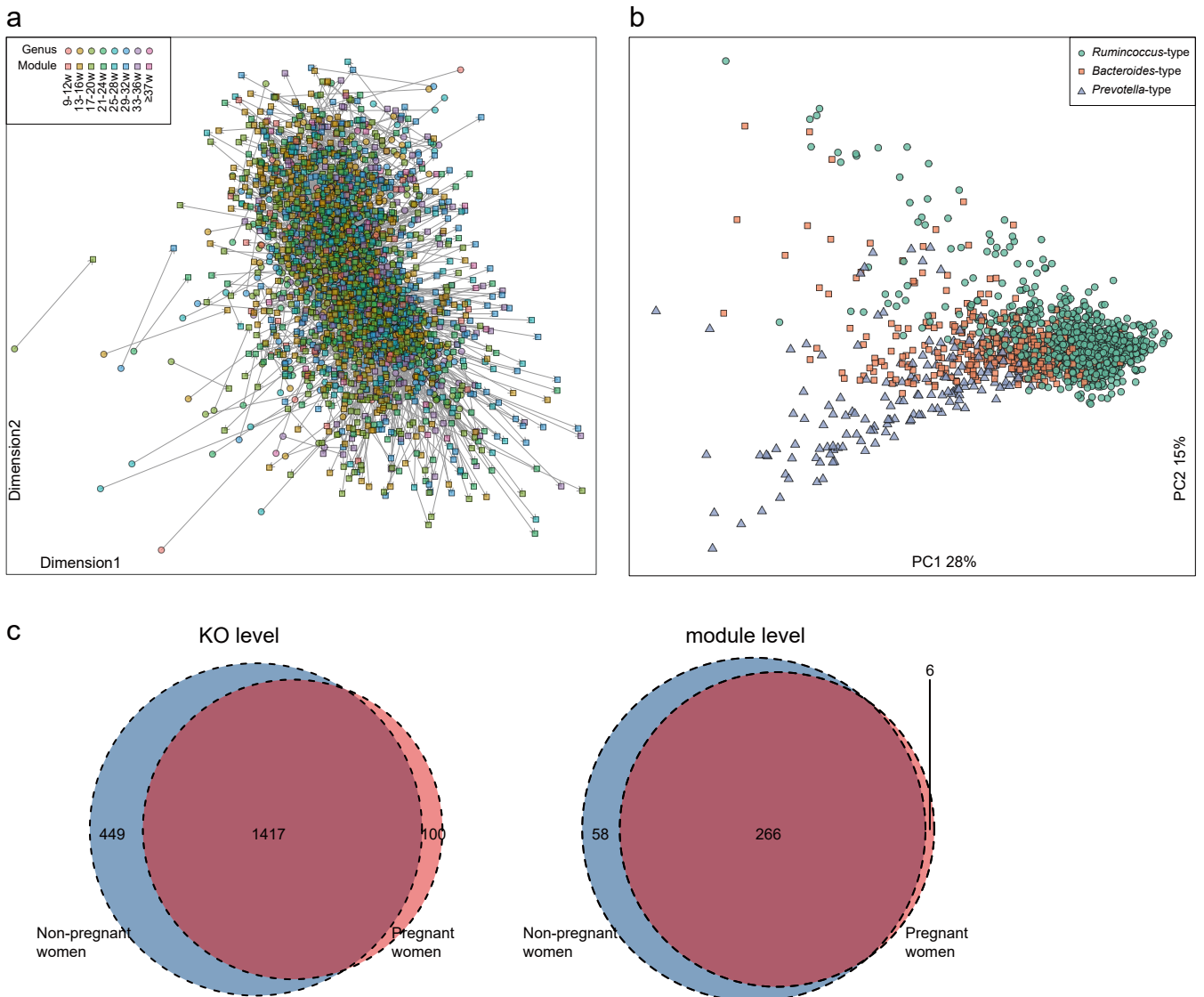
Supplementary Information



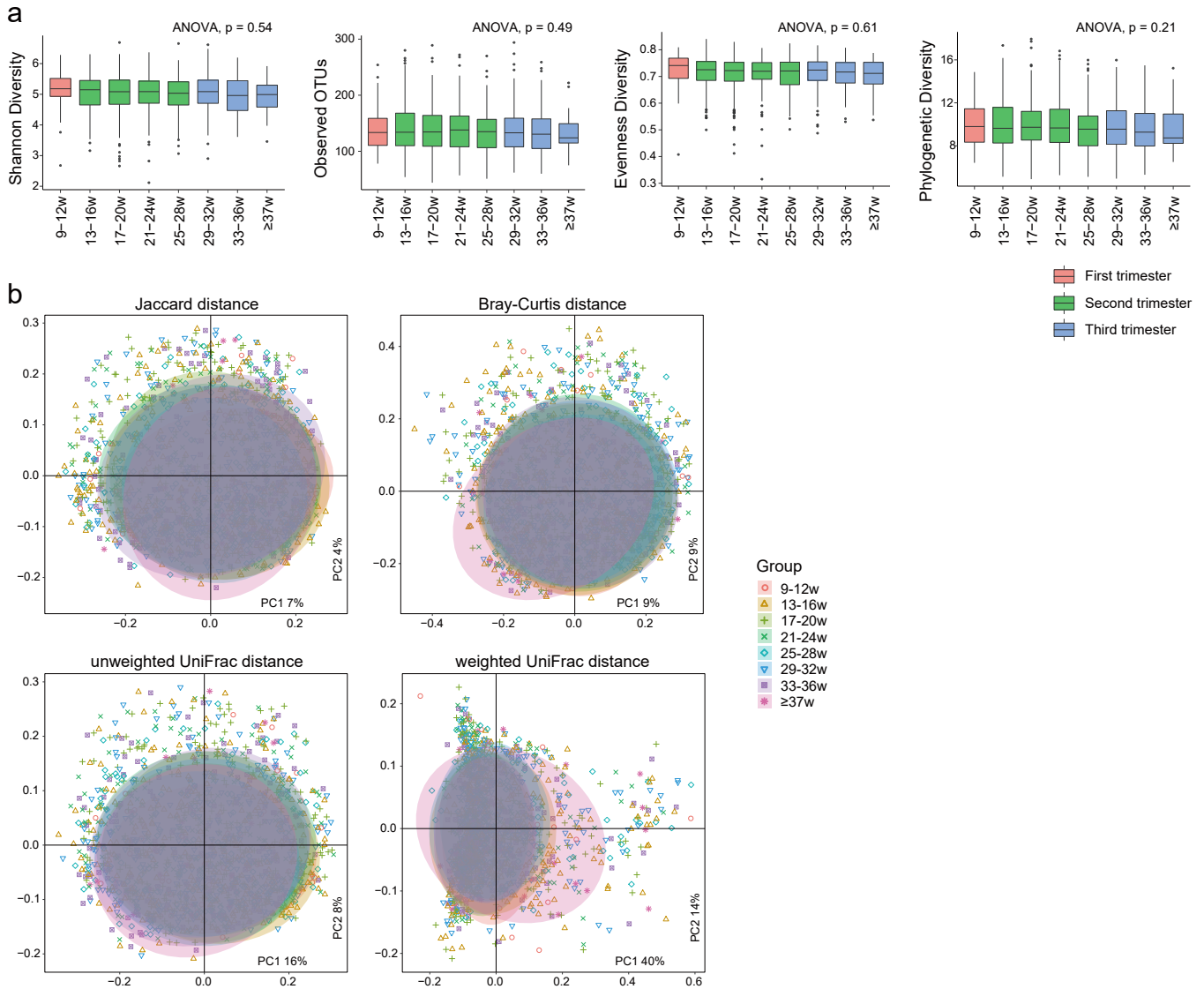
Supplementary Fig. 1. Composition of the pregnant women's gut microbiota at the phylum level.



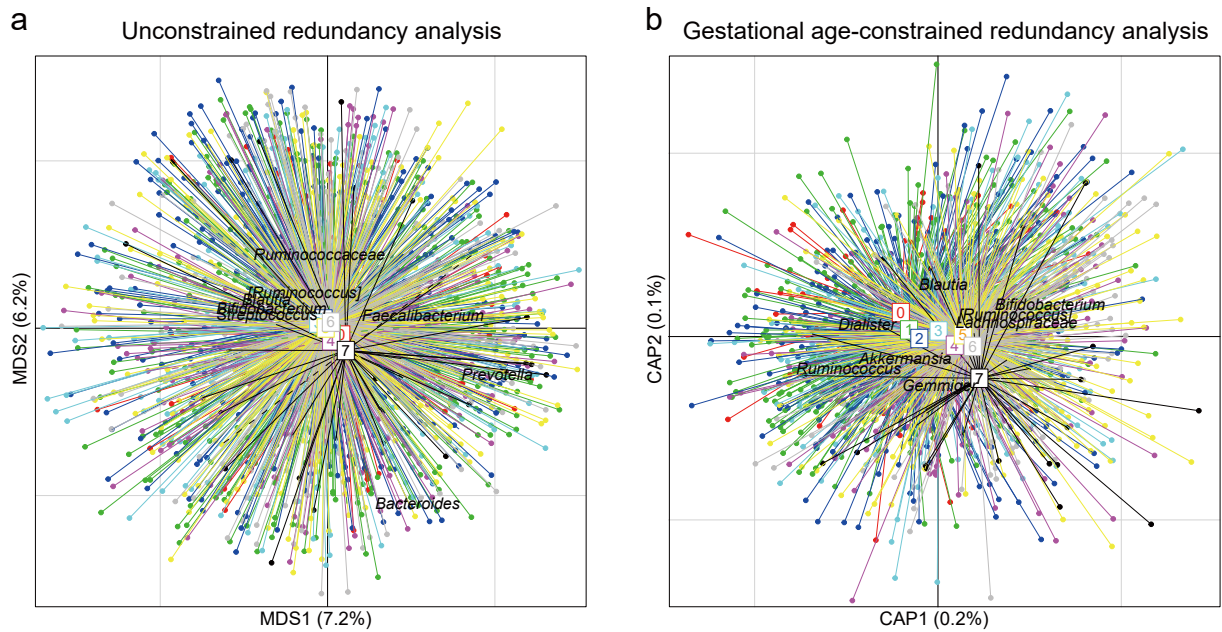
Supplementary Fig. 2. Distribution of OTUs that significant differed in relative abundance among the 8 gestational stages.



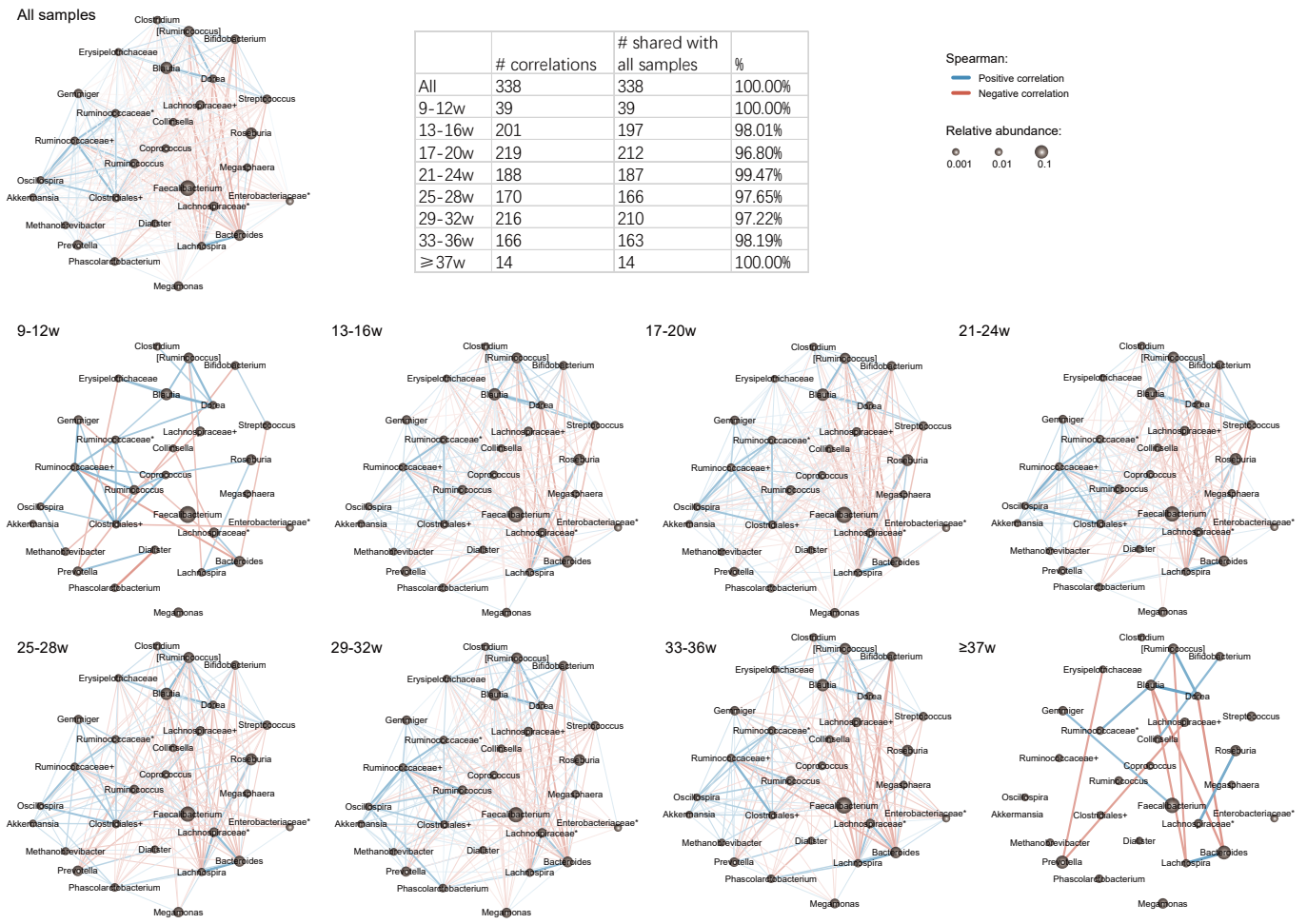
Supplementary Fig.3. The pregnant women's functional microbiome. **a** Procrustes analysis between microbial compositional and functional microbiomes. **b** Enterotype stratified the functional microbiome in pregnant women. Principal coordinates analysis (PCoA) based on the Bray-Curtis distance of KO profiles of pregnant women was shown. **c** Shared KO functional orthologs (left panel) and modules (right panel) between pregnant and nonpregnant women.



Supplementary Fig.4. Comparison of microbiota diversity among different gestational stages. **a** α -diversity comparison. The colors represented the first (red), second (green), and third (blue) trimesters of the samples of pregnant women. **b** PCoA analysis base on 4 β -diversity matrixes.

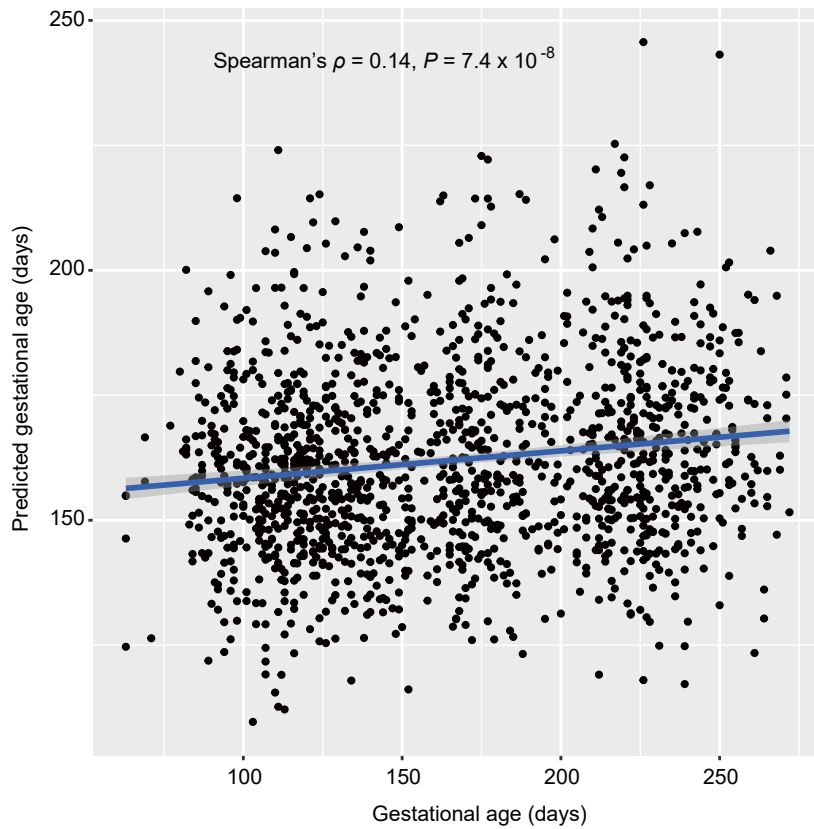


Supplementary Fig.5. Redundancy analysis of the gut microbiome of pregnant women. Unconstrained (**a**) and gestational-age constrained (**b**) redundancy analyses (RDA) was performed based on Bray-Curtis distance between microbial genera. Display of the unconstrained RDA was shown on sample scores on the primary and second multidimensional scales (MDS1 and MDS2), while display of the constrained RDA was shown on sample scores on the primary and second constrained axes (CAP1 and CAP2). Lines connected samples taken at the same gestational stages.

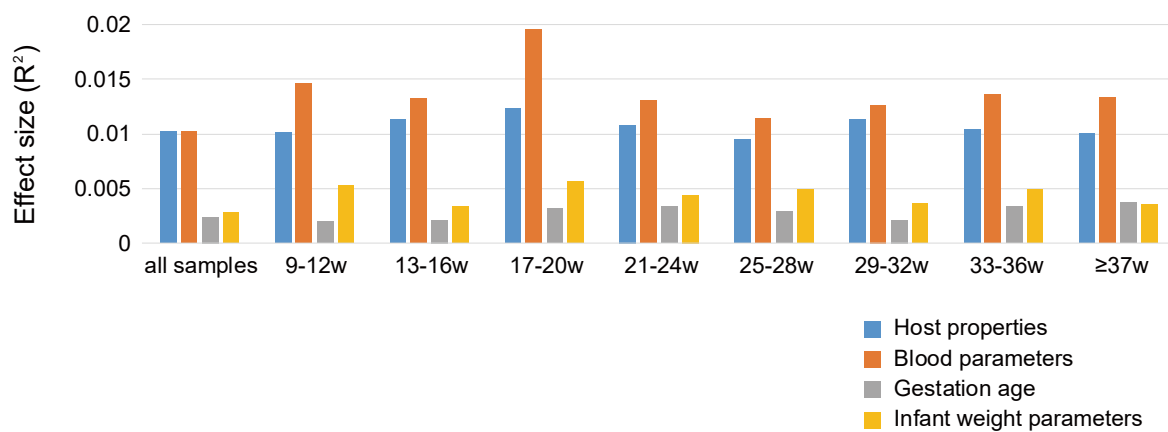


Supplementary Fig.6. Correlation network of the dynamics of 29 core genera.

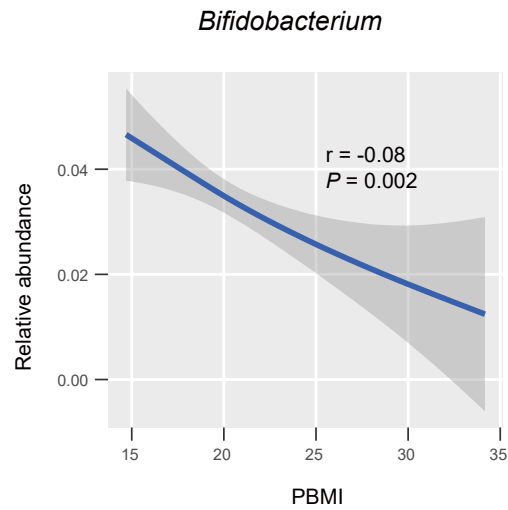
Correlation analysis was conducted on 29 core genera with average relative abundance >0.5% for all individuals or a subset of individuals at each gestational stage (Spearman's rank correlation coefficient test, $q \leq 0.05$). Blue line indicated positive correlation, and red line indicated negative correlation. Line color depth and width were proportional to degrees of the correlation. The table showed numbers of shared positive and negative correlation networks between genera for all individuals and individuals at each gestational stage.



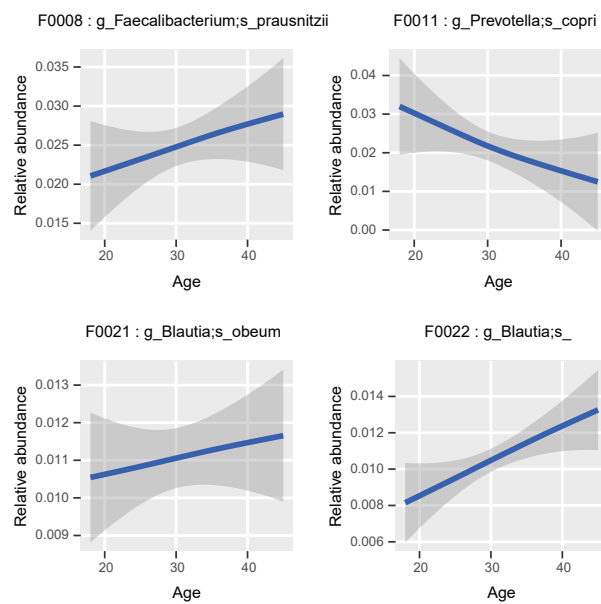
Supplementary Fig.7. Predicting the women's gestational age based on 11 gestational-age-associated genera.



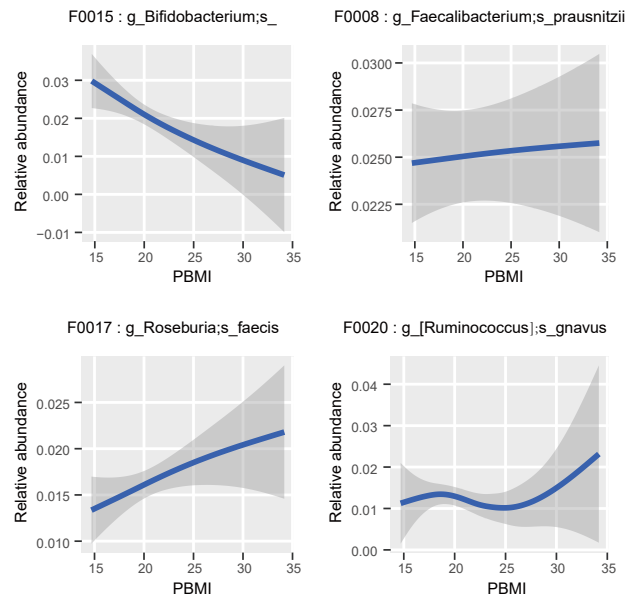
Supplementary Fig.8. The explicable variations of different categories of parameters for microbial community variation. Effect size was estimated using the function `adonis` with the default parameters in R.



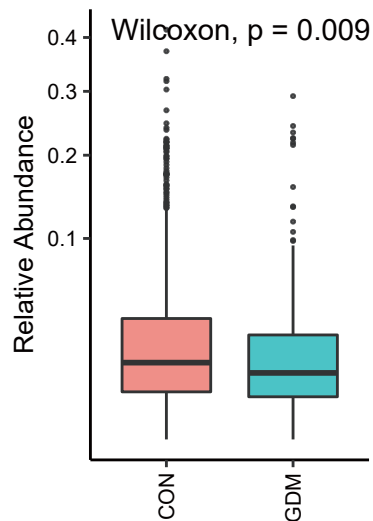
Supplementary Fig.9. Smooth curve based on the relative abundance of *Bifidobacterium* and pre-pregnancy body mass index (PBMI) of individuals. Smooth curve was formed using the function `geom_smooth` with the default parameters in R. The relationship and statistical significance between two data were determined by Spearman's rank correlation coefficient test.



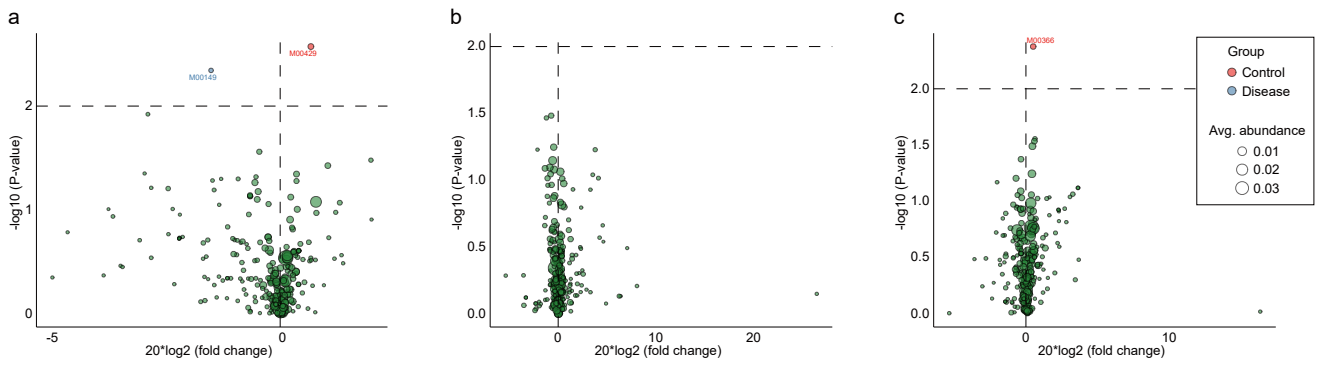
Supplementary Fig.10. Smooth curve based on the relative abundance of OTU and women's age. Smooth curve was formed using the function `geom_smooth` with the default parameters in R.



Supplementary Fig.11. Smooth curve based on the relative abundance of OTU and women's pre-pregnancy body mass index (PBMI). Smooth curve was formed using the function `geom_smooth` with the default parameters in R.



Supplementary Fig.12. The comparison of the relative abundance of genus *Streptococcus* between non-GDM and GDM women.



Supplementary Fig.13. The comparison of KEGG module-level D composition between control and disease group. **a** non-GDM versus GDM. **b** non-hepatopathy versus hepatopathy. **c** non-thalassemia versus thalassemia.